Journal of Inclusion Phenomena and Macrocyclic Chemistry (2006) 55:173–183
DOI 10.1007/s10847-005-9034-5

Aggregation and Adsorption Properties of Tetramethylsulfonatoresorcinarenes and Their Associates with Nonionogenic Guest Molecules in Aqueous Solutions

JULIA E. MOROZOVA[1], ELLA KH. KAZAKOVA[1,*], EDUARD PH. GUBANOV[1], NELLY A. MAKAROVA[1], VICTOR P. ARCHIPOV[2], TATJANA V. TIMOSHINA[1], ZAYMIL SH. IDIJATULLIN[2], WOLF D. HABICHER[3] and ALEXANDER I. KONOVALOV[1]

[1]*A.E. Arbizov Institute of Organic and Physical Chemistry RAS, Arbuzova Street 8, 420088, Kazan, Russia* [2]*S.M. Kirov Kazan State Technological University, K. Marks Street 68, 420015, Kazan, Russia;* [3]*Technical University of Dresden, Momsenstrasse 13, D-01062, Dresden, Germany*

(Received: 3 August 2005; in final form: 19 October 2005)

Key words: adsorption, aggregation, diffusion, amphiphils, host–guest complexes, resorcinarenes, surface tension

Abstract

Present paper reports on tensiometric studies of tetramethylsulfonatoresorcinarenes **1** and **2** with nonionogenic guests **3** and **4**, pyrimidin derivative and *O,O*-dymethyl-1,1-dimethyl-3-oxobutylphosphonate, respectively. Association of resorcinarenes with these guests leads to dramatic change of adsorption characteristics of their solutions. $CCMs_1$ of associates (**1&3**, **1&4**, **2&3**, and **2&4**) are lower and the estimated surface activity, as well as the height of adsorption layers are higher than for individual substances. Aggregation of compounds **1**–**4** and association of **1** with **3** and **4** in solution were confirmed by ^{1}H NMR spectra and studied by diffusion NMR with impulse magnetic field gradient.

Introduction

Both natural and synthetic amphiphils are known to reduce surface tension of aqueous solutions through formation of ordered layers at the phase boundary and micelle-like structures at the bulk of solution. Amphiphilic calixarenes and resorcinarenes with hydrophobic aromatic cavity can additionally form inclusion complexes. As it was shown in [1], complexation of macrocycles located on the phase boundary substantially differs from that in the bulk of solution.

It has been reported in ref. [2] that dodecylthiol cyclotetramer of resorcinol immobilized on gold surface possess sufficient affinity towards number of guests present in diluted solution. The same resorcinarene in chloroform solution of these guests did not form any inclusion complexes except for with glutaric acid. To explain these observations authors suggested that aggregation of amphiphilic macrocycle into reversed micelles in solution hinder formation of inclusion complexes. Similarly, it has been demonstrated in [3] that addition of certain sugars, to aqueous solutions alter pressure-area isotherms of multilayered Langmuir–Blodgett films prepared from resorcinol–dodecanal cyclotetramer and deposited on electrodes, this in turn affects response of electrode.

Here we present detailed study of surface activity and adsorption parameters of two tetramethylsulfonatoresorcinarenes **1** and **2** and their associates with nonionogenic compounds **3** and **4** (Figure 1). The latter are biologically active compounds [4] and examination of their binding with water-soluble container molecules is of substantial interest in regards to development of selective drug delivery. Both **3** and **4** can take part in multiple donor–acceptor interactions with resorcinolarenes [5–10]. In pyrimidin derivative **3**, H-acceptor centers are represented by four heteroatoms, whereas CH-bonds of two methyl substituents are potential H-donors capable also of dispersion interactions. *O,O*-dimethyl-1,1-dimethyl-3-oxobutyl phosphonate (keto-phosphonate, DDOBP) **4** of spherical shape has dimensions matching resorcinarene cavity size (ca. 8.5 Å, cavity – ca. 6×14 Å). This substrate has several H-acceptor, five H-donor, and four methyl groups with potential to dispersion and CH–π interactions. Phosphorus atom provides relatively rigid configuration and increase acidity of the nearby CH_2-groups.

Experimental

Tetramethylsuldonatoresorcinarenes **1** and **2** were synthesized according to [5], pyrimidin derivative **3** and

* Author for correspondence. E-mail: ella@iopc.knc.ru

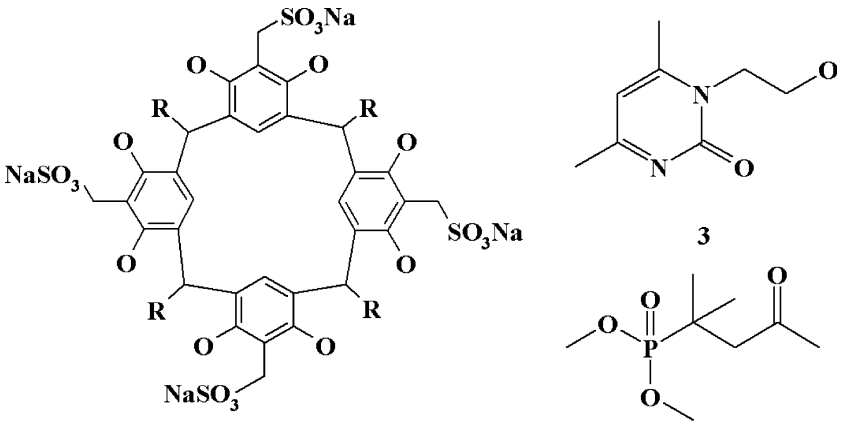

Figure 1. Structure of hosts **1** and **2** and guests **3** and **4**.

O,*O*-dimethyl-1,1-dimethyl-3-oxobuthylphosphonate **4** were a kind gift of Prof. V.S. Resnik and Dr. A.A. Muslinkin.

^{1}H and ^{13}C NMR spectra were recorded with a Bruker-MSL 300 spectrometer with the working frequency of 300.13 MHz with DSS as an external reference.

Surface tension measurements in aqueous solutions

Surface tension of solutions of **1**–**4** and their mixtures were determined according to Wilhelmy method for platinum plate [11]. To equilibrate the samples prior to measurements they were left at room temperature for 72 h. The standard deviation of surface tension from the mean values was less than ± 0.1 dyn cm^{-1}. CCM_1, value of maximum surface absorption (Γ_∞), surface activity $(\sigma - \sigma_0)/CMC_1$, and free energy of micellization (ΔG^0_m) were found from recorded surface tension isotherms $\sigma(\ln C)$ by applying standard procedure based on Gibbs equation [11] and using least square method for determining derivatives from the linear ranges of the isotherms for $C < CCM_1$. Surface area per molecule (S_m), thickness of absorption layers (δ) were determined according to:

$$S_m = \frac{1}{\Gamma_\infty \cdot N_A} \text{ and } \delta = \frac{M \cdot \Gamma_\infty}{\rho},$$

where T is temperature in K, M is molecular mass or amphiphil, and N_A is Avogadro number. Density of compounds **1**, **2**, **1&3**, and **1&4** was determined as described below and calculation of Γ_∞ and S_m were used to verify its reliability.

$$\Gamma_\infty = \frac{1}{S_m \cdot N_A} = \left(\frac{M}{\rho}\right)^{-\frac{2}{3}} \cdot N_A^{-\frac{1}{3}} \qquad (1)$$

Viscosymetry of aqueous solutions of **3** *and* **4**

Relative viscosity of **3** and **4** was determined with Ubellodes' viscosimeter [11] using molar ratio of 1:4 for respective substrate and Na_2SO_4. The standard deviation of relative viscosity from the mean values was less than ± 0.7.

Diffusion studies of aggregation properties of **1**–**4** *and associates* **1&3** *and* **1&4**

High resolution FT–NMR with impulse gradient of magnetic field was used to study aggregation properties of compounds **1**–**4** [12]. Aggregate dimensions were estimated based on the changes of their hydrodynamic radii calculated from Stocks–Einstein equation:

$$R_i = kT/6\pi\eta D_i,$$

where k is Boltzmann constant, T is temperature in K, η is dynamic viscosity coefficient, D_i is diffusion coefficient of aggregates, and R_i is hydrodynamic radius of aggregates.

Diffusion coefficients (D_i) and hydrodynamic radii (R_i) of compounds **1**–**4** were determined based on measurements performed on adapted NMR spectrometer Tesla BS-567A with working frequency of 100 MHz at 30 °C in D_2O solutions according to [13]. For associates **1&3** and **1&4** concentration of **1** was 2.0×10^{-1} M and concentrations of **3** and **4** were varied at the ranges of $5.0 \times 10^{-2} \div 4.0 \times 10^{-1}$ M and $2.0 \times 10^{-1} \div 8.0 \times 10^{-1}$ M, respectively. Diffusion coefficient of water (D_W) was determined from the signals of residual water with reliability of obtained values of 5–7%. Interactions of micellar aggregates with each other in concentrated solutions were corrected with specially introduced correction ϕ depending on aggregate content in solution [14].

Theoretical volumes of resorcinarene molecules (V) were calculated as:

$$V = \frac{M}{\rho N_A},$$

where M is a molar mass of amphiphil, ρ is density (see below), and N_A is Avogadro number. Volumes of molecules **3** and **4** were calculated according to the method

Table 1. Theoretical volumes (V) and effective radii (r) of molecules **1–4**

Compound	V, Å^3	r, Å
1	1480	7.1
2	1810	7.6
3	158	3.4
4	177	3.5

of atomic increments described elsewhere [15]. Theoretical volumes (see Table 1) of these molecules then were used for calculation of $\phi = VN_AC$.

Corrections ϕ allowed to correct determination of hydrodynamic radius (R_i) of molecules **1–4** and were, in turn, used to estimate aggregation number N:

$$N = \frac{4}{3}\pi R^3/V$$

Theoretical volume of molecules (V) were also used to calculate effective radii of molecules **1–4**:

$$r = \sqrt[3]{\frac{3V}{4\pi}}$$

Preparation of adducts 1&3, 1&4, 2&3 and 2&4

Ablation of water from solutions **1&3**, **1&4**, **2&3**, and **2&4** prepared for surface tension measurements resulted in crystalline powders that did not melt below 350 °C and were characterized by individual spots on TCL plates.

*Synthesis of **1&3***. A mixture of 0.504 g (5.0×10^{-4} M) of **1** and 0.084 g (5.0×10^{-4} M) of **3** in 5 ml of water was kept at room temperature for 2 months. Solution was monitored by TCL with dioxane:water 10:1 eluent, R_f 0.75. After disappearance of free **3**, water was removed in vacuum and residue was thrice washed with chloroform and dried in vacuum (70 °C, 30 h). Obtained rose crystalline structure (yield 0.437 g, 74.32%) was characterized: m.p. > 300 °C, $C_{36}H_{36}O_{20}Na_4S_4{\cdot}C_8H_{12}O_2N_2$. Calculated, %: C 44.04, H 4.08, N 2.38, Na 7.82, S 10.88, found, % C 43.72, H 3.93, N 2.33, Na 7.51, S 10.35.

Determination of density of compounds **1**, **2**, **1&3** *and* **1&4**

Density was determined based on the mass ratio of investigated and displacing solutions taken at a given volume and at the same temperature. Prior to measurement investigates substance was pounded and annealed at 100 °C for 2 h and then cooled in desiccator filled with $CaCl_2$. Twenty-five milliliter densimeter was closed and weighted (m_1, 20 °C) and then half filled with investigated substance and weighted (m_2) and then filled with displacing substance – toluene. Displacing substance should have a high boiling point and posses good wetting properties towards the substance under investigation that should be insoluble in it. Densimeter was placed in vacuum-desiccator, where it was kept for 4 h to ablate air and then weighted (m_3). After that cleaned and empty densimeter was filled with toluene up to hairline, thermostated, and weighted (m_4). Density of investigated substance (ρ_{20}) was calculated as:

$$\rho_{20} = \rho_1 \frac{m_2 - m_1}{(m_4 - m_1) - (m_3 - m_2)}.$$

Density of displacing substance (ρ_1) at the temperature of the experiment was calculated as:

$$\rho_1 = \rho \frac{(m_4 - m_1)}{(m_5 - m_1)},$$

where m_5 is a mass of densimeter filled with water and ρ is density of water at the temperature of experiment. Obtained density values are an average of three parallel measurements and for **1**, **2**, **1&3**, and **1&4** were found to be 1.58 ± 0.02, 1.44 ± 0.02, 1.56 ± 0.02, and 1.53 ± 0.01 g cm^{-3}, respectively.

Results

Two macrocyclic tetramethylsulfonatoresorcinarenes with methyl and penthyl lower rim substituents were recently studied as host molecules for a number of different substrates [5–10]. The macrocycles are well soluble in water, glycerin, and DMSO. In aqueous media they exist as tetra-anions and, as previously reported in [5], acidity of their OH-groups have following pK 9.0 ± 0.8; pK_2 9.3 ± 0.1; pK_3 10.8 ± 0.3; pK_4 10.6 ± 0.1. Spatial separation of hydrophilic and hydrophobic zones of resorcinarenes features their amphiphilic properties that reveal themselves in adsorption at solution/air interface and in formation of aggregates in the bulk of solution. Both of these processes were characterized by tensiometric measurements in aqueous solutions of **1** and **2** (Table 1). Measurements in aqueous solutions of **1** resulted in isotherm that indicates the absence of aggregation up to 6.41×10^{-2} M (ln C −2.75). CCM_1 for macrocycle **2** was found to be 8.87×10^{-4} M (ln C −7.02), which is in a good agreement with CCM_1 of 8.0×10^{-4} M obtained by conductometric titration [16].

Tensiometric studies of aqueous solutions of pyrimidine derivative **3** and ketophosphonate **4** gave surface tension isotherms typical for surfactants. In case of **3**, two extremes on isotherm correspond to the maximum of surface adsorption and CCM_1, respectively. The latter determined for **3** and **4** were found to be 0.123 M (ln C −2.1) and 0.459 M (ln C −0.78).

Table 2 summarizes characteristics of adsorption and micellization calculated based on isotherms of individual compounds **1–4**: value of maximum surface absorption (Γ_∞), surface activity ($(\sigma - \sigma_0)/CMC_1$, free energy of micellization (ΔG^0_m), thickness of absorption layers (□), and diameter of the hydrophilic area per one molecule (d).

The influence of association of resorcinarenes **1** and **2** with **3** and **4** on the surface activity of macrocycles was examined tensiometrically for respective equimolar (1:1)

Table 2. Adsorption and aggregation parameters of individual compounds **1**, **2**, **3**, and **4**

Compound		**1**	**2**	**3**	**4**
Concentration range of isotherm [M]		$9.91 \times 10^{-5} \div 0.198$ (ln C $-9.22 \div -1.62$)	$8.11 \times 10^{-5} \div 8.1 \times 10^{-3}$ (ln C $-9.42 \div -7.12$)	$0.008 \div 0.8$ (ln C $-4.83 \div -0.22$)	$0.025 \div 1$ (ln C $-3.69 \div 0$)
Γ_∞	Eexp	1.28×10^{-10}	1.43×10^{-10}	6.60×10^{-10}	2.97×10^{-10}
[mol cm^{-2}]	Calc[a]	1.60×10^{-10}	1.31×10^{-10}	4.74×10^{-10}	3.62×10^{-10}
cmc [M]		$(6.40 \pm 0.01) \times 10^{-2}$	$(8.90 \pm 0.01) \times 10^{-4}$	$(1.20 \pm 0.01) \times 10^{-1}$	$(4.60 \pm 0.01) \times 10^{-1}$
σ_{kkm} [dyn/cm^{-1}]		44.5	48.3	63.2	42.7
$(\sigma - \sigma_0)/cmc$		440	27,479	77	65
D [Å]	Exp	13	12	6	8
	Calc[a]	12	13	7	8
	MM + [b]	14	14	6	–
δ [Å]	Exp	8	12	8	6
	Calc[a]	8	11	6	7
	MM + [b]	5	10	3.5	–
ΔG^0_m [kJ mol^{-1}]		−16.8	−27.5	−15.2	−11.9

[a]Thermodynamic model, calculated according to Equation (1).
[b]Thikness of layer estimation (MM +).

solutions at the concentration range $9.9 \times 10^{-5} \div 2.0 \times 10^{-1}$ for **1&3** (**4**) ($8.1 \times 10^{-5} \div 8.1 \times 10^{-3}$ for **2&3** (**4**)). Obtained surface tension isotherms are presented on the Figure 2 and adsorption parameters are given in Table 3.

To elucidate aggregation of compounds **1**–**4**, a high resolution NMR with Fourier-transformation and impulse field gradient [12] was used. This method allows selective determination of diffusion coefficients of single

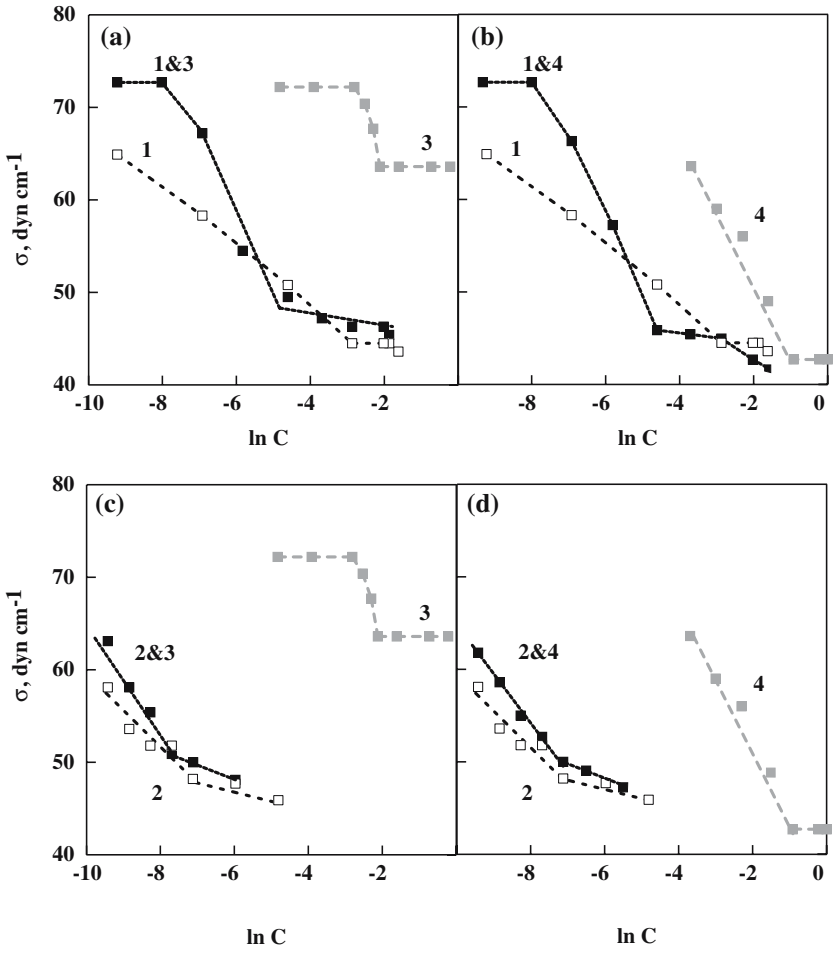

Figure 2. Surface tension isotherms (20 °C): A: **1**, **3,** and **1&3**; B: **1**, **4** and **1&4**; C: **2**, **3,** and **2&3**; D: **2**, **4**, and **2&4**.

Table 3. Adsorption and aggregation parameters of aqueous solutions of **1&3**, **1&4**, **2&3**, and **2&4**, 20 °C

Compound		**1&3**	**1&4**	**2&3**	**2&4**
Γ_∞ [mol cm^{-2}]	Exp	4.6×10^{-10}	3.2×10^{-10}	2.7×10^{-10}	2.1×10^{-10}
	Calc[a]	1.4×10^{-10}	1.4×10^{-10}	1.2×10^{-10}	1.2×10^{-10}
Cmc [M]		$(4.30 \pm 0.01) \times 10^{-3}$	$(1.10 \pm 0.01) \times 10^{-2}$	$(4.60 \pm 0.01) \times 10^{-4}$	$(6.60 \pm 0.01) \times 10^{-4}$
σ_{kkm} [dyn cm^{-1}]		50.0	45.8	50.9	50.4
$(\sigma - \sigma_0)/cmc$		5227	2386	47,275	33,658
D [Å]	Exp	7	8	9	10
	Calc[a]	12	12	13	13
δ [Å]	Exp	35	25	26	21
	Calc[a]	11	11	12	12
ΔG^0_m [kJ mol^{-1}]		−23.5	−21.0	−29.1	−28.2

[a]Thermodynamic model, calculated according to Equation (1).

components in solutions, e.g. of solvent and dissolved substance. Diffusion coefficients (D_w of water and D_i of compounds **1**–**4**) along with calculated hydrodynamic radii R for different concentrations are listed in Table 4 (for calculations see ref. [13]). Similarly, diffusion coefficients and hydrodynamic radii were determined for **1&3** and **1&4** (Table 5). Indexes $_1$ and $_G$ for D_1, R_1 and D_G, R_G denote respectively host **1** and guest **3** or **4** characteristics.

Recently we described formation of inclusion complex between **1** and **4** [10]. TLC of mixture **1&3** indicated the absence of free **3** in it. NMR investigation of complexation between **1** and **3** was carried in D_2O and DMSO solutions. Observed *CIS* are listed in Table 6 (for full information on NMR data see also Tables A1–A7 in Appendix A). For complexes of **2** with **3** and **4** ^{13}C NMR spectra in D_2O were rather complex for interpretation and for complete characterization of these complexes ^1H and ^{13}C NMR spectra were recorded in DMSO-d_6. This solvent is quite unusual for NMR study but it was the only one that provided sufficient solubility of the complexes.

Amphipilic resorcinarenes **1** and **2** can be approximated to polyelectrolytes known for their effect on surface activity of neutral surfactants [11]. The influence of **1** and **2** on aggregation and adsorption of **3** and **4** was examined by viscosymetry. In the course of this experiment a charge born by **1** and **2** was modeled by respective amount of Na_2SO_4 added to solutions of **3** and **4** (Figure 3). Recorded values of relative viscosity show that addition of electrolyte reduces CCM_1 for both **3** and **4**. In the presence of Na_2SO_4 CCM_1 for **3** and **4** was found to be $(1.20 \pm 0.05) \times 10^{-1}$ M (ln C −2.12) *versus* $(2.7 \pm 0.05) \times 10^{-1}$ M for pure solutions of **3** and **4**.

Discussion

As illustrated by Table 1, the surface activities of resorcinarenes **1** and **2** differ sufficiently due to the presence of 16 additional CH_2-groups at the lower rim of the aromatic cavity in the latter. Good agreement between experimental and calculated values of the maximum surface adsorption (Γ_∞) and of experimental,

Table 4. Diffusion coefficients D_i and hydrodynamic radii R_i of compounds **1**–**4** in aqueous solutions

Compound	C, M	D_w, 10^{-5} cm^2/c	D_i, 10^{-5} cm^2/c	R_i, 10^{-10} m
1	3.2×10^{-1}	1.27 ± 0.06	(8.04 ± 0.56)×10^{-2}	9.7 ± 0.9
	2.0×10^{-1}	1.67 ± 0.08	(1.55 ± 0.11)×10^{-1}	9.8 ± 0.9
	1.0×10^{-1}	1.81 ± 0.09	(2.18 ± 0.15)×10^{-1}	9.8 ± 0.9
	5.0×0^{-2}	2.10 ± 0.10	(3.20 ± 0.22)×10^{-1}	8.9 ± 0.8
	2.5×10^{-2}	2.07 ± 0.10	(3.36 ± 0.23)×10^{-1}	9.3 ± 0.8
	1.2×10^{-2}	2.30 ± 0.11	(4.38 ± 0.31)×10^{-1}	7.5 ± 0.7
2	3.2×10^{-2}	1.92 ± 0.10	(9.16 ± 0.64)×10^{-2}	32.5 ± 2.9
	1.6×10^{-1}	2.02 ± 0.10	(1.05 ± 0.07)×10^{-1}	30.4 ± 2.7
3	1.2	1.59 ± 0.08	(4.38 ± 0.31)×10^{-1}	4.8 ± 0.4
	1.0	1.58 ± 0.08	(4.47 ± 0.31)×10^{-1}	5.1 ± 0.4
	4.0×10^{-1}	1.86 ± 0.09	(5.60 ± 0.39)×10^{-1}	5.3 ± 0.5
	2.0×10^{-1}	1.92 ± 0.10	(6.10 ± 0.42)×10^{-1}	5.2 ± 0.5
	1.5×10^{-1}	1.95 ± 0.10	(6.70 ± 0.47)×10^{-1}	4.8 ± 0.4
4	8.0×10^{-1}	1.62 ± 0.08	(4.88 ± 0.34)×10^{-1}	4.9 ± 0.4
	4.0×10^{-1}	1.78 ± 0.09	(5.52 ± 0.39) ×10^{-1}	5.2 ± 0.5
	2.0×10^{-1}	1.85 ± 0.09	(6.13 ± 0.43) × 10^{-1}	5.1 ± 0.4

Table 5. Diffusion coefficients and hydrodynamic radii of host **1** (D_1 and R_1) and guests **3** and **4** (D_G and R_G) in aqueous solutions of associates **1&3** and **1&4** (0.2 M)

	C_G, M	D_w, 10^{-5} cm^2/c	D_1, 10^{-5} cm^2/c	D_G, 10^{-5} cm^2/c	R_1, Å	R_G, Å
1&3	4.0×10^{-1}	1.50 ± 0.07	$(1.31 \pm 0.09) \times 10^{-1}$	$(2.60 \pm 0.16) \times 10^{-1}$	7.3 ± 0.6	7.9 ± 0.6
	2.0×10^{-1}	1.58 ± 0.08	$(1.42 \pm 0.10) \times 10^{-1}$	$(2.94 \pm 0.18) \times 10^{-1}$	7.0 ± 0.6	7.5 ± 0.6
	1.0×10^{-1}	1.61 ± 0.08	$(1.46 \pm 0.10) \times 10^{-1}$	$(3.02 \pm 0.18) \times 10^{-1}$	7.0 ± 0.6	7.6 ± 0.6
	5.0×10^{-2}	1.63 ± 0.08	$(1.60 \pm 0.11) \times 10^{-1}$	$(2.98 \pm 0.18) \times 10^{-1}$	6.5 ± 0.6	7.8 ± 0.6
1&4	8.0×10^{-1}	1.39 ± 0.07	$(1.28 \pm 0.09) \times 10^{-1}$	$(2.82 \pm 0.17) \times 10^{-1}$	8.0 ± 0.7	5.9 ± 0.5
	4.0×10^{-1}	1.49 ± 0.07	$(1.50 \pm 0.11) \times 10^{-1}$	$(3.39 \pm 0.20) \times 10^{-1}$	7.5 ± 0.6	5.9 ± 0.5
	2.0×10^{-1}	1.48 ± 0.07	$(1.49 \pm 0.10) \times 10^{-1}$	$(3.42 \pm 0.20) \times 10^{-1}$	7.9 ± 0.7	6.4 ± 0.5

calculated and model values of the surface area per molecule (d) indicate formation of a densely packed layer at the aqueous solution/air interface. The difference between model and experimental thickness of an adsorption layer (δ) indicates deviation of this layer from monomolecular structure. The CCM_1 and $(\sigma - \sigma_0)/CCM_1$ values give quantitative estimation of the surface activity of **1** and **2**. The free energy of micellization calculated from them is twice higher for **2** than for **1**, ΔG^0_m of which is close to those of **3** and **4** having a low surface activity and CCM_1 in decimolar range.

For **3** the surface area per molecule of 6 Å and the thickness of the layer of 8 Å (for a monolayer taking into account only hydrophobic part of molecule it is 3.5 Å) along with the deviation of experimental Γ_∞ from respective calculated value suggest formation of a bi-layered structure at the solution/air interface. For neither of the examined individual substances **1**–**4**, it is possible to declare formation of a monomolecular adsorption layer at the phase boundary. However, taking into account good agreement between the experimental and calculated surface area per molecule it is possible to suggest formation of a staggered phase boundary layer that will correspond to the experimental value of its thickness.

In case of the resorcinarenes such model closely resembles the host–guest packing, where methyl groups or aliphatic chains of the lower layer molecules interact with π-fragments and polar groups of the upper layer oriented 'to aqueous solution'. For guest molecules **3** and **4** suggested bilayer packing is stabilized by multi-point hydrogen bonding between CH-protons and polar domains of the layer.

While tensiometric determination of the surface activity characteristics is based on measurements of the phase boundary layer properties, nothing is known about processes taking place at the same time in the bulk of solution at concentrations close to CCM_1. To elucidate these processes a high resolution NMR spectroscopy with Fourier-transformation and impulse gradient of field was used. This method allows estimation of the aggregation number, N, corresponding to a number of individual molecules in an associate existing in the bulk of solution.

As it is clear from the Table 3, hydrodynamic radii of **1** starts to deviate from its effective radii (7.5 Å) at concentrations sufficiently lower than CCM_1 determined tensiometrically $(1.20 \pm 0.05) \times 10^{-2}$ M). The aggregation numbers of 2–3 correspond to this process. Hydrodynamic radii of **2** (R 30 Å) is sufficiently higher than its effective radii (r 7.6 Å, see Exp. Part, Table 1) and slightly varies at the concentration range of $1.6 \times 10^{-2} \div 3.2 \times 10^{-2}$ M, where calculated aggregation number N is 60–70.

Bulk aggregation properties of **3** and **4** are rather weak. Experimental hydrodynamic radii of 5 and 4.5 Å for them are close to effective radii of 3.4 and 3.5 Å at the concentration range of $1.5 \times 10^{-1} \div 1.2$ M and $2.0 \times 10^{-1} \div 8.0 \times 10^{-1}$ M, respectively. Obtained aggregation numbers for them were 3–4.

Association of **1** and **3** in aqueous solution was determined with the help of NMR (see Table 6) based on up-field CIS of protons of **3** caused by inclusion of it into aromatic cavity. NMR spectra of **1&3** in DMSO feature significant down-field shifts of protons indicating donor–acceptor interactions of **3** with peripheral groups of **1**. Association of **1** and **4** was earlier discussed in detail in ref [8].

Table 6. Complexation induced shifts (CIS) of protons of guests **3** and **4** ($\Delta\delta$, ppm) in complexes with **1** and **2** in D_2O and DMSO solutions

	D_2O	DMSO-d_6	D_2O	DMSO-d_6
	1&3		**2&3**	
$(CH_3)C$–N	−0.12	0.31	0.70	[a]
$(CH_3)C$=N	−0.24	0.17	0.65	[a]
CH	−0.30	0.47	−0.38	[a]
CH_2N	−0.10	0.04	0.11	[a]
CH_2O	−0.07	0.13	−0.23	[a]
	1&4		**2&4**	
$(CH_3)_2C$	−0.18[c]	0.33	[a]	0.33
$CH_3C(O)$	−0.07[c]	0.37	0.03	0.35
$CH_2C(O)$	−0.14[c]	0.37	0.02	0.36
$(CH_3O)_2P$	−0.05[c]	0.30	0.10	0.30
$\Delta\delta$ ^{31}P NMR	0.420[c]	−1.65	–	2.33

[a]The observed *CIS* ±0.01 ppm.
[b]No observed shift.
[c]The values of *CIS* was taken from ref. [8].

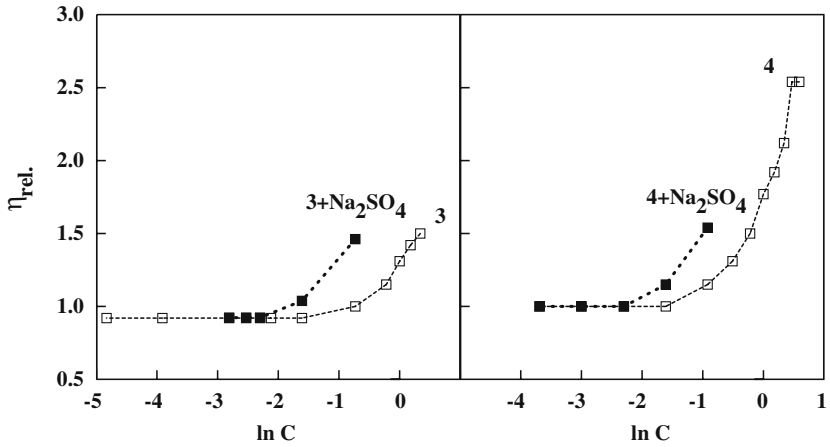

Figure 3. Dependence of relative viscosity on concentration for aqueous solutions of **3** and **4** in the presence and absence of Na_2SO_4.

Complexes of macrocycle **2** were isolated from aqueous solutions that according to TLC contained no free **3** or **4**. ^1H NMR spectra of these complexes in D_2O demonstrated general broadening of signals and both up- and down-field shifts of guest protons (Tables 6, A2, and A4). ^1H and ^{13}C NMR spectra of the same complexes in DMSO, the only solvent providing good solubility of the complexes, do not show any up-field shift of guests protons typical for inclusion complexes (Tables A3 and A5). Based on earlier studies of solvent influence on complexes of resorcinarenes [10], it was suggested that in DMSO binding of **3** and **4** is realized predominantly via multipoint interaction with peripheral groups of resorcinarenes, whereas in water, dominating hydrophobic favor inclusion of guests in resorcinarene cavity.

Tensiometric studies of complexes of **3** and **4** with **1** and **2** summarized in Table 3 clearly indicate the absence of additivity of the properties related to surface activity. For **1&3** and **1&4** surface activity is 12 and five times higher that for individual **1** and 68 and 37 times higher than for individual **3** and **4**. The thickness of the surface layer calculated from the experimental data was found to be 35 and 25 Å, respectively, and CCM_1 for these complexes are six to 10 times lower that of **1**. Similar tendencies were observed for **2&3** and **2&4** (Table 3), however CCM_1 these associates do not increase so dramatically due to the high surface activity of **2** itself. For both **1** and **2** the effect of **3** on surface activity of complexes is more pronounced than that of **4**.

Diffusion properties of single components in solutions of complexes are listed in Table 4. Hydrodynamic radius of macrocycle in inclusion complex is reduced till its effective radii, so that it can be suggested that whereas in solutions of pure **1** di- and trimerization takes place, in solution of complexes **1&3**

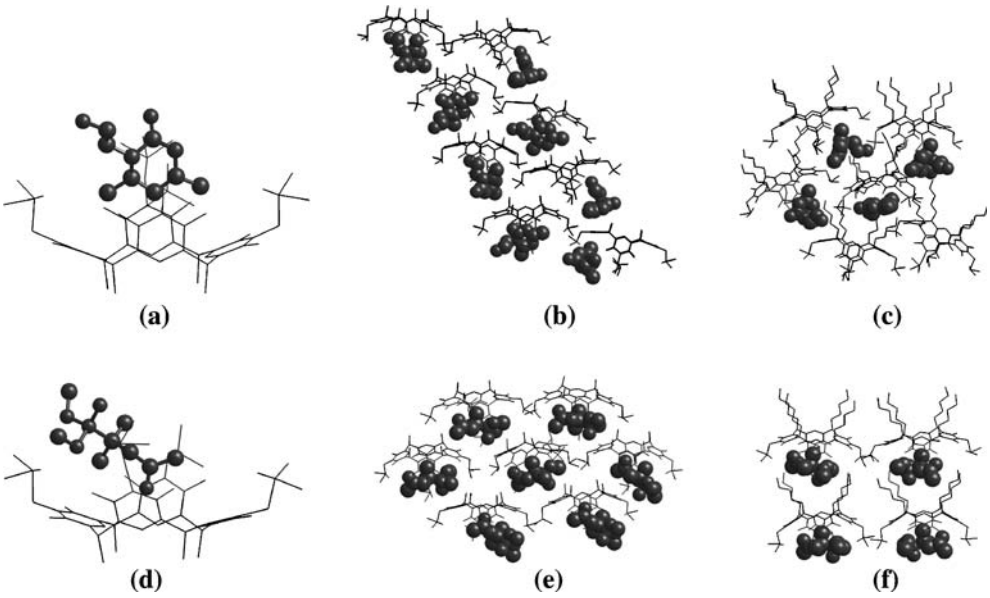

Figure 4. Models of complexes (A – **1&3**, D – **1&4**) and absorption layers at the aqueous solution/air interface (B – **1&3**, C – **2&3**, E – **1&4**, F–**2&4**).

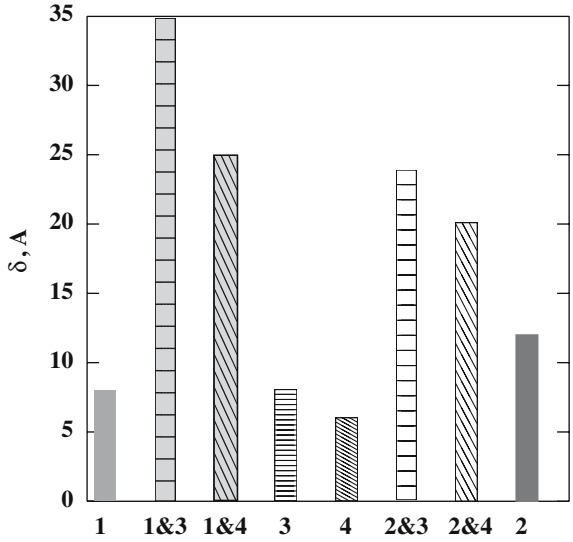

Figure 5. Diagram of height of the adsorption layers of compounds **1**–**4** and their complexes.

and **1&4** monomeric **1** forms exclusively 1:1 complexes. This suggestion is in a good agreement with the increase of hydrodynamic radii (from 4.8 and 5.1 to 7.8 and 6.4) of guests **3** and **4** included into aromatic cavity.

Viscosymetric measurements with solutions of **3** and **4** in the presence of Na_2SO_4 modeling charge of **1** and **2** (Figure 3) show only two-fold reduction of CCM_1 compare to pure solutions of the guests. Thus, indicating a minor impact of ion–dipole interactions into decrease of CCM_1 of the guests solutions in the presence of the hosts. Presence of **1** and **2** decrease CCM_1 28 and 267 times for **3** and 41 and 692 times for **2**, pointing to the major role of weak noncovalent interactions in increase of the surface activity of these complexes. Apparently, hydratation of polar zone of macrocycles facing aqueous solution compete with multipoint binding of guests decreasing dipole moment of the boundary layer and promoting further aggregation with the lower layer of host molecules.

It was reported in ref. [1] on molecular recognition at the water/air interface resulting in formation of mixed adsorbed layers. Whereas intermolecular association in diluted solutions corresponds to relatively low CCM_1, at the phase boundary they increase due to formation of highly ordered layer composed of interacting host and guest molecules. The authors, therefore, suggested that significant increase in electrostatic interactions at the phase boundary is caused by rather close packing of hydrophobic fragments having low dielectric constant. Such arrangement creates favorable conditions for all kinds of noncovalent interactions including electrostatic. Similar interactions can take place in the bulk of solution at concentrations close to CCM_1, where guests could be bound by surface of a large host aggregate [17]. In the same way, trying to develop a consistent model of phase boundary layer in solutions of complexes of **1** and **2** with **3** and **4**, we resorted to molecular modeling by MM+ force field method (HyperChem® Release 5.0, N 500-10001026, Hypercube Inc.) to provide visual representation of the complexes (Figure 4) taking into account parameters of the adsorption layers obtained experimentally. It was concluded that solution/air interface of **1&3** consists of four layers of suggestively arranged **1** incorporating **3** in the intermolecular gaps, while for **1&4** and **2&3** it is represented by alike tri- and for **2&4** bilayered structures.

Conclusions

Present work demonstrated that amphiphilic tetraanionic host molecules **1** and **2** in aqueous solutions form inclusion complexes with nonionogenic compounds **3** and **4**. The binding is accompanied by nonadditive increase of the surface activity of both host and guest (Figure 5). Presumably, decrease of polarity and increase of hydrophobic surface of inclusion complexes as compared to individual hosts and guests enhances driving force of formation of multilayered structure at the aqueous solution/air interface.

Acknowledgments

Financial support was provided by the grants of the RFBR N 03-03-33080 and Programs 7 and 8 of the Division of Chemistry and Material Science RAS.

Appendix A

Table A.1. ^{1}H, ^{13}C NMR-data for **1**, **3** and **1&3** in D_2O

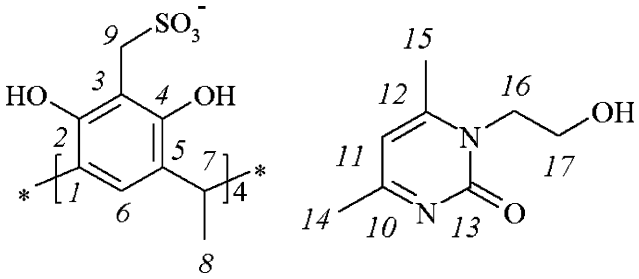

NN	1	3	1&3
^{1}H, δ, ppm (J, Hz) [$\Delta\delta$, ppm]			
CH	4.47 q (7.07)	–	4.56 q (6.85) [+0.09]
ArH	6.72 s	–	6.76 s [+0.04]
$ArCH_2S$	4.33 s	–	4.29 s [−0.04]
CH_3	1.55 d (7.50)	–	1.50 d (7.06) [−0.05]
$(CH_3)C–N$	–	2.34 s	2.22 s [−0.12]
$(CH_3)C=N$	–	2.51 s	2.27 br d [−0.24]
CH	–	6.52 s	6.22 s [−0.30]
CH_2N	–	3.94 t (5.44)	3.84 t (5.32) [−0.10]
CH_2O	–	4.18 t (5.43)	4.11 t (5.25) [−0.07]
^{13}C, ppm (J, Hz) [$\Delta\delta$, ppm]			
$C^{1,5}$	127.66	–	128.60 [+1.09]
$C^{2,4}$	150.60	–	151.29 [+0.69]
C^{3}	110.12	–	110.89 [+0.79]
C^{6}	125.06	–	125.91 [+0.85]
C^{7}	30.52 d	–	32.42 [+1.90]
C^{8}	19.05	–	20.61 [+1.56]
C^{9}	46.94	–	48.18 [+1.24]
C^{10}	–	161.95	160.94 [−1.01]
C^{11}	–	109.85	109.24 [−0.61]
C^{12}	–	159.51	158.70 [−0.81]
C^{13}	–	176.94	216.47 [+39.53]
$C^{14,15}$	–	21.19, 24.66	20.98 [−0.21], 31.37 [+6.71]
C^{16}	–	49.13	50.16 [+1.03]
C^{17}		59.66	59.12 [−0.43]

Table A.2. ^{1}H, ^{13}C NMR-data for compounds **1**, **3** and **1&3** in DMSO-d_6

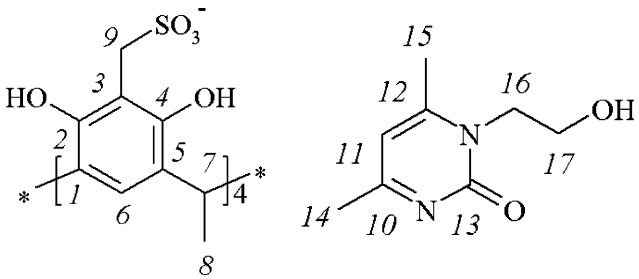

NN	1	3	1&3
^{1}H, δ, ppm (J, Hz) [$\Delta\delta$, ppm]			
CH	4.47 q (7.07)	–	4.46 q (7.15) [−0.01]
ArH	7.45 s	–	7.45 s [0.00]
$ArCH_2S$	3.86 s	–	3.86 s [0.00]
CH_3	1.75 d (7.50)	–	1.72 d (7.02) [−0.03]
$(CH_3)C–N$	–	2.18 s	2.49 s [+ 0.31]
$(CH_3)C=N$	–	2.41 s	2.58 s [+0.17]
CH	–	6.25 s	6.72 s [+0.47]
CH_2N	–	3.65 t	3.69 t (5.15) [+0.04]
CH_2O	–	3.95 t (5.46)	4.08 t (5.13) [+0.13]
^{13}C, ppm (J, Hz) [$\Delta\delta$, ppm]			
$C^{1,5}$	125.92	–	125.73 [−0.19]
$C^{2,4}$	149.74	–	149.57 [−0.17]
C^{3}	109.16	–	108.99 [−0.17]
C^{6}	122.99	–	122.82 [−0.17]
C^{7}	29.65 d	–	28.38 [1.27]
C^{8}	20.31	–	20.15 [−0.16]
C^{9}	46.94	–	47.97 [−0.17]
$C^{1°}$	–	158.47	a
C^{11}	–	105.06	106.68 [+1.62]
C^{12}	–	155.99	a
C^{13}	–	173.25	168.59 [−4.65]
$C^{14,15}$	–	19.91; 24.18	20.33 [+0.42]; 21.30 [−2.88]
C^{16}	–	47.20	48.95 [+1.75]
C^{17}		57.93	57.33 [−0.60]

[a]The signal was overlapped with one of $^{2,4}C$

Table A.3. ^{1}H NMR-data for **2, 3** and **2&3** in D_2O

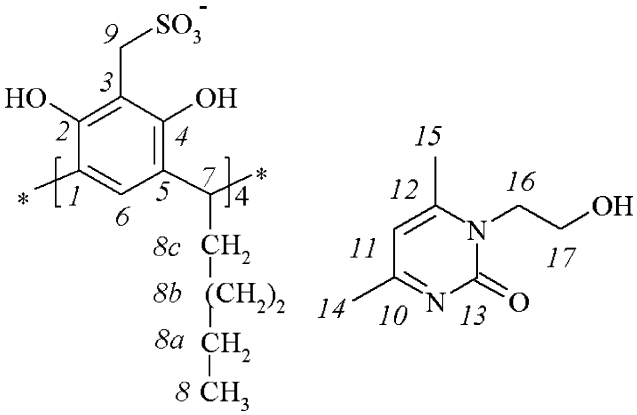

NN	2	3	2&3
^{1}H, δ, ppm (J, Hz) [$\Delta\delta$, ppm]			
CH_3	0.83 br t	–	0.83 br s [0.00]
$(CH_2)_3$	1.25–1.37 m	–	1.22 br s
$CHC\underline{H}_2$	1.99 br s	–	2.06 br s [+0.07]
$ArCH_2S$	3.68 q	–	3.93 br s [+0.25]
CH	4.38 br t	–	4.38 br t [0.00]
ArH	7.02 br s	–	7.17 br s [+0.15]
OH	A	–	a
$CH_3C–N$	–	2.34 s	3.04 br s [+0.70]
$CH_3C=N$	–	2.51 s	3.26 br d [+0.65]
CH_2O	–	3.92 t (5.44)	3.69 br t [−0.23]
CH	–	6.53 s	6.15 br s [−0.38]

Table A.3. Continued

NN	**2**	**3**	**2&3**
CH_2N	–	4.19 t (5.43)	4.30 br t [+0.11]
CH_2O	–	3.92 t (5.44)	3.69 br t [−0.23]
OH	–	a	a

[a]No observed shift.

Table A.4. ^1H ^{13}C NMR-data for **2, 3** and **2&3** in DMSO-d_6

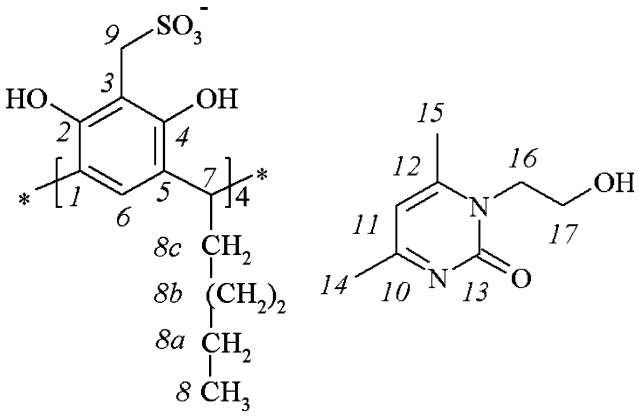

NN	**2**	**3**	**2&3**
^1H, δ, ppm (J, Hz) [$\Delta\delta$, ppm]			
CH_3	0.83 t	–	0.87 t [−0.01]
$(CH_2)_3$	1.24–1.20 m	–	1.23–1.32 m
$CHC\underline{H}_2$	1.99 br s	–	2.24 q [−0.03]
$ArCH_2S$	3.89 s	–	3.86 s [−0.03]
CH	4.25 t	–	4.21 t [−0.04]
ArH	7.29 s	–	7.34 s [+0.05]
OH	9.69 br s	–	9.72 s [+0.03]
CH_3C–N	–	2.18 s	2.19 [+0.01]
CH_3C=N	–	2.41 s	2.41 [+0.00]
CH_2O	–	3.95 t (5.46)	3.94 t (5.23) [−0.01]
CH	–	6.24 s	6.25 s [+0.01]
CH_2N	–	3.65 t (5.21)	3.64 q (5.02) [−0.01]
CH_2O	–	3.95 t (5.46)	3.94 t (5.23) [−0.01]
OH	–	5.00 br s	4.99 t [−0.01]
^{13}C, ppm (*J*, Hz) [$\Delta\delta$, ppm]			
$C^{1,5}$	127.34	–	124.71 [−2.63]
$C^{2,4}$	152.09	–	149.93 [−2.16]
C^3	110.33	–	108.91 [−1.42]
C^6	125.14	–	122.92 [−2.22]
C^7	36.37	–	32.42 [+1.90]
C^8	15.41	–	13.98 [−1.43]
C^{8a}	23.95	–	22.17 [−1.78]
C^{8b}	33.68, 31.28	–	33.06 [−0.62], 31.57 [+0.29]
C^{8c}	28.97	–	27.78 [−1.19]
C^9	49.06	–	48.15 [−0.91]
$C^{1°}$		158.47	158.69 [+0.22]
C^{11}		155.99	156.16 [+0.17]
C^{12}		105.06	105.29 [+0.23]
C^{13}		173.25	173.41 [+0.16]
$C^{14,15}$		19.91, 24.18	20.05 [+0.16], 24.28 [+0.14]
C^{16}		47.20	47.32 [+0.12]
C^{17}		57.93	57.97 [+0.04]

Table A.5. ^1H, ^{13}C NMR-data for **1**, **4** and **1&4** in DMSO-d_6

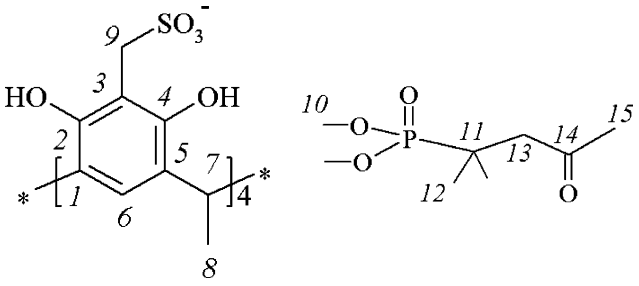

	1	**4**	**1&4**
^1H, δ, ppm (*J*, Hz) [$\Delta\delta$, ppm]			
CH	4.47 q (7.07)	–	4.48 q [−0.01]
ArH	7.46 s	–	7.45 s [−0.01]
$ArCH_2S$	3.87 s	–	3.85 s [−0.02]
CH_3	1.72 d (7.50)	–	1.72 d (7.20) [0.00]
OH	9.58 s	–	9.62 s [0.04]
$(CH_3)_2C$	–	0.86 d (11.6)	1.19 d (17.1) [+0.33]
$CH_3C(O)$	–	1.73 d (11.8)	2.10 s [+0.37]
$CH_2C(O)$	–	2.21 d (10.85)	2.58 d (10.77) [+0.37]
$(CH_3O)_2P$	–	3.36 d (10.38)	3.66 d (10.27) [+0.30]
δ ^{31}P NMR, ppm	–	36.02	34.37 [–1.65]
^{13}C, δ, ppm (*J*, Hz) [$\Delta\delta$, ppm]			
$C^{1,5}$	125.92	–	125.71 [−0.21]
$C^{2,4}$	149.74	–	149.55 [−0.19]
C^3	109.16	–	109.00 [−0.16]
C^6	122.99	–	122.78 [−0.21]
C^7	29.65 d	–	28.36 [1.29]
C^8	20.31	–	20.12 [−0.19]
C^9	46.94	–	47.96 [1.02]
C^{10}		55.15	52.74 [−2.41]
C^{11}		36.40	34.58 [−1.82]
C^{12}		22.71	20.86 [−1.85]
C^{13}		49.02	46.72 [−2.30]
C^{14}		185.79	208.60 [+22.81]
C^{15}		33.40	31.91 [−1.49]

Table A.6. ^1H NMR-data for **2**, **4** and **2&4** in D_2O

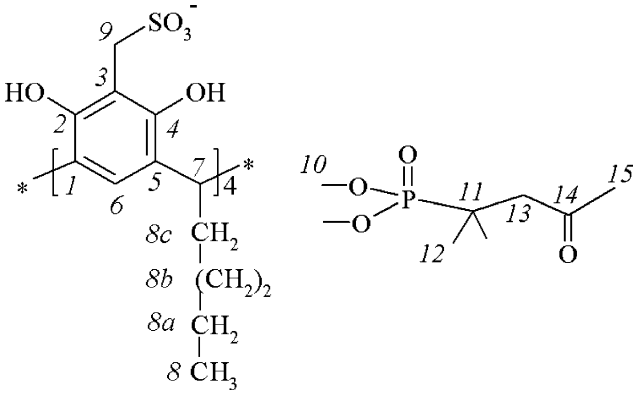

Table A.6. Continued

	2	4	2&4
^{1}H, δ, ppm (J, Hz) [$\Delta\delta$, ppm]			
CH_3	0.83 br t	–	0.82 br s [−0.01]
$(CH_2)_3$	1.24–1.20 m	–	1.25 br d
$CHC\underline{H}_2$	1.99 br s	–	1.99 br s [0.00]
$ArC\underline{H}_2S$	3.68 q	–	3.82 br d [+0.14]
CH	4.38 br t	–	4.37 br t [−0.01]
ArH	7.02 br s	–	7.02 br s [0.00]
OH	[a]	–	[a]
$(CH_3)_2C$	–	1.26 d (17.39)	1.25 d [−0.01]
$CH_3C(O)$	–	2.10 s	2.23 br s [+0.03]
$CH_2C(O)$	–	2.69 d (12.96)	2.71 br s [+0.02]
$(CH_3O)_2P$	–	3.77 d (10.23)	3.67 d [+0.10]

[a]No observed shift.

Table A.7. ^{1}H, ^{13}C NMR-data for **2, 4** and **2&4** in DMSO-d_6

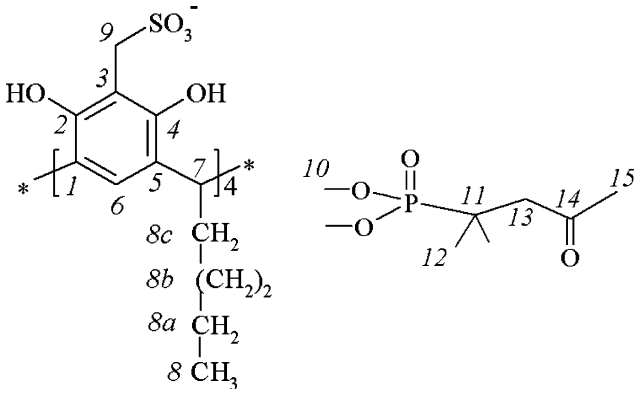

	2	4	2&4
^{1}H, δ, ppm (J, Hz) [$\Delta\delta$, ppm]			
CH_3	0.88 t	–	0.86 t [−0.02]
$(CH_2)_3$	1.25–1.37 m	–	1.29–1.31 m
$CHC\underline{H}_2$	2.27 q	–	2.23 q [−0.04]
$ArC\underline{H}_2S$	3.89 s	–	3.85 s [−0.04]
CH	4.25 t	–	4.20 t [−0.05]
ArH	7.29 s	–	7.33s [+0.04]
OH	9.69 br s	–	9.71s [+0.02]
$(CH_3)_2C$	–	0.86 d (11.6)	1.19 d (11.8) [+0.33]
$CH_3C(O)$	–	1.73 d (11.8)	2.08 s [+0.35]
$CH_2C(O)$	–	2.21 d (10.85)	2.57 d (10.77) [+0.36]
$(CH_3O)_2P$	–	3.36 d (10.38)	3.66 d (10.22) [+0.30]
δ ^{31}P NMR, ppm	–	36.50	38.83 [+2.33]
^{13}C, ppm (J, Hz) [$\Delta\delta$, ppm]			
$C^{1,5}$	127.34		124.70 [−2.64]
$C^{2,4}$	152.09		149.93 [−2.16]
C^3	110.33		108.92 [−1.41]
C^3	125.14		122.89 [−2.25]
C^6	36.37		34.12 [−2.25]
C^7	15.41		13.98 [−1.43]
C^8	23.95		22.17 [−1.78]
C^{8a}	33.68		33.05[−0.63]
C^{8b}	31.28		31.57 [+0.29]
C^{8c}	28.97		27.78 [−1.19]
C^9	49.06		48.15 [−0.91]
C^{10}		55.15	52.91[−2.24]; 52.82 [−2.33]
C^{11}		36.40	34.64 [−1.58]
C^{12}		22.71	20.93 [−7.78]
C^{13}		49.02	46.78 [−2.24]
C^{14}		185.79	206.42 [+20.63]
C^{15}		33.40	31.98 [−1.42]

References

1. M. Onda, K. Yoshihara, H. Koyano, K. Ariga, and T. Kunitake: *J. Am. Chem. Soc.* **118**, 8524 (1996).
2. H. Adams, F. Davis, and Ch.J.M. Stirling: *J. Chem. Soc., Chem. Commun.* **21**, 2527 (1994).
3. K. Kurihara, K. Ohto, Y. Tanaka, and Y. T. Aoyama Kunitake: *J. Am. Chem. Soc.* **113**, 444 (1991).
4. G.A. Izmailov, S.G. Izmailov, L.Kh. Mavzyutov, S.M. Gorbunov, G.B. Evranova, T.F. Rakhmatullina-Miller, V.S. Reznik, and A.A. Muslinkin: *RU Pat. 2019176* (1994); V. Yu. Tereshchenko, R.N. Gabbasov, G.A. Izmailov, S.G. Izmailov, V.S. Reznik, and A.A. Muslinkin: *RU Pat. 2073514* (1997); I.V. Zaikonnikova, I.A. Andreevna, A.V. Mazurin, V.V. Talantov, T.V. Bulatova, V.F. Zhavoronkov, V.P. Pankova, S.V. Maltsev, B.A. Arbuzov, A.O. Vizel, A.A. Muslinkin, M.R. Rokitsky, I.G. Gilmutdinov and L.S. Raimova: *WO Appl. 8502770* (1985); V.I. Danilov, Kh.M. Shulman, I.V. Zaikonnikova, I.A. Studentsova, R.Kh. Khafizyanova, I.A. Latfullin, Yu.E. Moskalenko, G.B. Vajnshtejn, B.A. Arbuzov, A.O. Vizel, A.A. Muslinkin, E.A. Gurylev, V.N. Nabiullin, A.I. Minkevich, S.I. Nizamutdinov, A.V. Gorozhanin, G.E. Dudenas, I.I. Makauskas and A.S. Puodzhyunas: *SU Pat. 1754111* (1992).
5. E.Kh. Kazakova, N.A. Makarova, A.Yu. Ziganshina, L.A. Muslinkina, A.A. Muslinkin, and W.D. Habicher: *Tetrahedron Lett.* **41**, 10111 (2000).
6. E.Kh. Kazakova, A.U. Ziganshina, J.E. Morozova, L.A. Muslinkina, N.A. Makarova, A.R. Mustafina, and W.D. Habicher: *J. Incl. Phenom.* **43**, 65 (2002).
7. A.R. Mustafina, V.V. Skripacheva, N.A. Makarova, E.Kh. Kazakova, V.E. Kataev, L.V. Ermolaeva, and W.D. Habicher: *J. Incl. Phenom.* **43**, 77 (2002).
8. E.Kh. Kazakova, N.A. Makarova, A.I. Rakhmatullin, L.A. Muslinkina, and A.A. Muslinkin: *J. Inclusion Phenom.* **36**, 153 (2000).
9. N.A. Makarova, E.Kh. Kazakova, Z.Ph. Salahutdinova, K.M. Enikeev, and A.I. Konovalov: *Zh. Obshch. Kimi.* **72**, 1652 (2002).
10. N.A. Makarova, E.Kh. Kazakova, J.E. Morozova, W.D. Habicher, and A.I. Konovalov: *Zh. Obshch. Kimi.* **73**, 1441 (2003).
11. D. Myers: *Surfaces, Interfaces and Colloids: Principles and Applications*, VCH, Wiley (1999).
12. B. Lindman and P. Stilbs, In S.E. Friberg, and P. Bothorel (eds.), *Microemulsions: Structure and Dynamics*, Chemical Rubber, Boca Raton, FL (1987), p. 320.
13. V.D. Fedotov, Yu.F. Zuev, V.P. Archipov, and Z.Sh. Idiyatullin: *Appl. Magn. Reson.* **11**, 7 (1996).
14. A. Blaaderen, J. Peetermans, G. Maret, and J.K.G. Dhont: *J. Chem. Phys.* **96**, 4591 (1992); M. Tokuyama and I. Oppenheim: *Phys. Rev.* **E 50**, R16 (1994); H.N.W. Lekkerkerker and J.K.G. Dhont: *J. Chem. Phys.* **80**, 5790 (1984).
15. J.T. Edward: *J. Chem. Educ.* **47**, 261 (1970).
16. R.R. Amirov, Z.T. Nugayeva, A.R. Mustafina, S.V. Fedorenko, V.I. Morozov, E.Kh. Kazakova, W.D. Habicher, and A.I. Konovalov: *Colloids Surf. A: Physicochem. Eng. Aspects* **240**, 35 (2004).
17. Y. Oishi, Y. Torii, M. Kuramori, K. Suehiro, K. Ariga, K. Taguchi, A. Kamino, and T. Kunitake: *Chem. Lett.* **6**, 411 (1996); Y. Oishi, Y. Torii, T. Kato, M. Kuramori, K. Suehiro, K. Ariga, K. Taguchi, A. Kamino, H. Koyano, and T. Kunitake: *Langmuir* **13**, 519 (1997).